N_2-Filled Hollow Glass Beads as Novel Gas Carriers for Microcellular Polyethylene

Lijie Dong,[1,2] Jing Huang,[1] Rui Li,[1] Yi Zhang,[1] Minxuan Pan,[1] Chuanxi Xiong[1]

[1]*School of Materials Science and Engineering, Wuhan University of Technology, Wuhan 430070, China*
[2]*Max-Planck Institute for Polymer Research, Mainz 55128, Germany*

Received 5 December 2008; accepted 23 June 2009
DOI 10.1002/app.31013
Published online 19 August 2009 in Wiley InterScience (www.interscience.wiley.com).

ABSTRACT: N_2-filled hollow glass beads (HGB) were first used as novel gas carriers to prepare microcellular polymers by compression molding. Dicumyl peroxide was acted as crosslink agent to control the produced microcellular structure of low density polyethylene (LDPE)/HGB. The effect of temperature, pressure and the content of gel on the embryo-foaming, and final-foaming structure are investigated. Scanning electronic microscopy shows that the average cell size of microcellular LDPE ranges from 0.1 to 10 μm, and the foam density is about 10^9–10^{11} cells/cm^3. A clear correlation is established between preserving desirable micromorphologies of microcellular LDPE in different processing stage and tuning processing factors. The pertinent foaming mechanism of microcellular materials foamed with HGB is proposed. Because of the good mechanical strength, low density, weak water-absorption, and excellent heat insulate ability, microcellular LDPE has great potential application in energy building materials. © 2009 Wiley Periodicals, Inc. J Appl Polym Sci 114: 4030–4035, 2009

Key words: microcellular LDPE; compression molding; morphology; structure-property relations; thermal properties

INTRODUCTION

Microcellular materials are a kind of advanced materials for many industrial applications, which exhibit average cell size ranging from 1 to 10 μm in diameter and foam density in the range of 10^9–10^{15} cells/cm^3. Owing to superior properties such as high thermal stability, low thermal conductivity and dielectric constant, and excellent mechanical properties, they have been widely applied in the fields of architecture, medical treatment, automobile industry, hydrogen storage materials, and packaging.[1–3]

Since microcellular foams have paid more attention in recent years,[4,5] relative microcellular foaming theories have been developed for approaching toward novel microcellular materials with the uniform distribution of cells and the excellent mechanical strength. The classic nucleation theory assumes that bubble nucleation is initiated by the formation of the critical size bubble, but it is limited because the energy required to form the critical bubble is ignored.[6–9] A gaseous bubble formation model and a vapor bubble formation model have been produced for the modified classic nucleation theory.[10,11] It is very nice that this model bridges the gap between the bubble embryo (a critical cluster) and the critical bubble. Moreover, macroscopic growing of gas bubbles had been intensively studied. Some of the earliest works were carried out in the 1950s by Epstein and Plesset[12] as well as Scriven.[13] Han and Yoo[14] provided a realistic model of structural foam expansion. In the late 1980s, Flumerfelt and coworkers[15,16] began development of a model that incorporated simultaneous nucleation and bubble growth.

Numerous techniques for preparing microcellular materials have been developed, which include chemical and physical foaming. The former has some distinguishing features in which it allows easy control of pore structure. Pore structure control is important to the thermal, mechanical property and performance of the microcellular materials in most cases.[17] However, chemical foaming method has shortcomings owing to additive foaming agents. These accessory foaming ingredients are sensitive to temperature, which cause the release of noxious gas, consequently, deteriorated gradually in foaming materials.

Recently, physical foaming techniques have attracted much attention because of their advantages in environmental benign and high bubble productivities.[18–21] No harmful additive is removed from the final product material, which make such microcellular material used in practical application. Stable gas, CO_2 or N_2, is commonly used as a blowing agent, which undergo a series of physical transition to

Correspondence to: C. Xiong (polymerlab@whut.edu.cn).
Contract grant sponsor: National Key Technology R&D Program of China; contract grant number: 2007BAE10B02.
Contract grant sponsor: National Natural Science Foundation of China; contract grant number: 50802068.

form bubbles. In this case, extrusion and injection molding are main approaches toward preparing microcellular materials, especially with supercritical CO_2. However, a shortcoming of such processing method is a quite long working period because the procedure included preparing of impact samples and swelling gas in the as-prepared impact samples melt or solution.

In this article, we have developed a simple and facile compression molding method to prepare microcellular materials, in which N_2-filled hollow glass beads (HGB) are used as gas carriers. Because of the watery melt of low density polyethylene (LDPE) at high temperature, Dicumyl peroxide (DCP) are used as crosslink agent for immobilizing bubbles. The processing undergoes preliminary mixed (premixed) stage for dispersing HGB in LDPE matrix and foaming stage for formation of microcellular materials. By tuning the key processing parameters, controlled morphologies of produced microcellular LDPE in the two stages are obtained. Therefore, microcellular LDPE with the size of 0.1–10 μm and the foam density of 10^9–10^{11} cells/cm^3 is achieved.

MATERIALS AND EXPERIMENTAL

Materials

LDPE pellets, 18D, with 1.5 g/10 min of melt index and 0.918 g/cm^3 of density, were purchased from China Petroleum and Chemical Corporation. N_2-filled HGB with $\sim$ 45 μm in diameter were manufactured by Songlin (China). DCP produced from Lingfeng Chemical Reagent (China).

Preparation of microcellular LDPE

LDPE pellets and N_2-filled HGB were premixed at the melt temperature of LDPE. The procedure as follows: LDPE pellets were melted in XSS-300 Torque Rheometer at the rotator speed of 40 rpm for 4–5 min. Two suggestive temperatures were 130 or 150°C, respectively. Followed, the rotator speed decreased to 25 rpm and quantitative N_2-filled HGB were added into the melted LDPE. In this stage, slow feeding speed plays a critical role to ensure lower-density HGB anchoring on the surface of LDPE melt. To immobile bubbles, proportional DCP was added into the melt LDPE/HGB mixture. The relative weight fraction of DCP was calculated at 0.2, 0.5, 1.0, 1.5, 2.0, and 2.5%, which aimed at obtaining desirable embryo-foaming morphology.

Microcellular foaming procedure was preformed immediately after premixed stage. Mixed LDPE/HGB composites were removed quickly as 4-mm-thick sheet mold and were hot-pressed at 160°C and 6 or 8 MPa for 8 min, and then the mold was rapidly depressurized by releasing pressure within 3–5 s. The resulting microcellular materials were taken from the mold after cooling.

Characterization

All produced sheets were cut into rectangular 100 mm × 10 mm × 4 mm bars and were further fractured in liquid nitrogen. Their cross-sections were coated with gold and were studied by scanning electronic microscopy, SEM (JEOL, JSM-5610LV). The morphologies of fracture surface, both embryo-foaming morphology and final-foaming structure, were observed by image analysis.

The gel content of the crosslink samples were calculated according to literary method.[22] The crosslink bars were cut into slivers and were extracted at 140°C for 24 h in the Soxhlet apparatus, and then further dried to constant weight. Xylene was used as extractor solvent. The gel content value φ was determined as the following equation: $\varphi = m_2 / m_1$, where m_1 and m_2 denoted the mass of original material and that of extracted sample, respectively.

The tensile strength and breaking elongation of foaming materials were obtained at the tensile rate of 250 mm/min by using RG-M-30A material testing machine. The Charpy nonnotch impact strength of microcellular LDPE was tested at the JB6 impact tester. The hardness of samples were measured by LX–A Shore durometer. The density of samples was calculated according to weighing method. Water absorption of microcellular LDPE after 24 h was measured. The thermal conductivity of produced samples was measured in KDR-1B Instantaneous Intelligent Thermal Conductivity Test Instrument, and the dimension of these samples were rectangular 130 mm × 50 mm × 4 mm.

RESULTS AND DISCUSSION

Morphology controlling in premixed stage and molding compression

Preserving embryo-foaming morphology in premixed stage and immobility of final-foaming structure in compression molding play critical roles for desirable produced microcellular LDPE, which depend strongly on key processing parameters, such as the premixed temperature, the processing pressure, and the content of DCP.

Controlled embro-foaming morphologies in premixed stage

The effect of premixed temperature on the embryo-foaming morphology is studied at constant rotor speed, as shown in Figure 1. Different embryo-

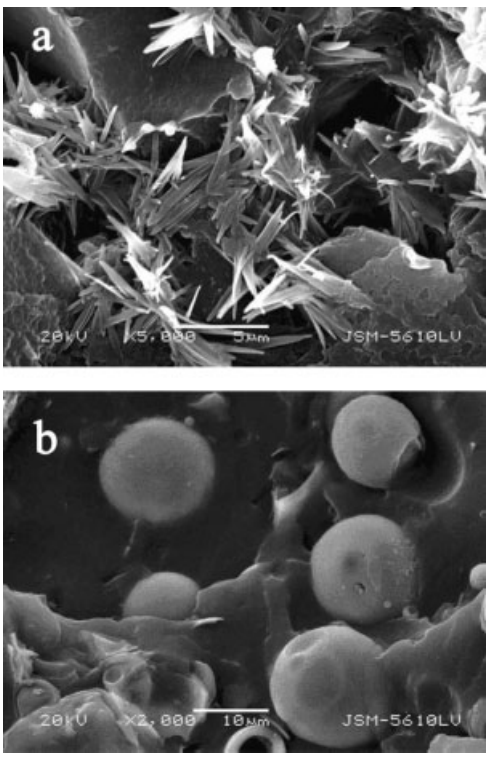

Figure 1 SEM images of LDPE/HGB in premixed stage at (a) 130°C and (b) 150°C (f_{HGB}: 10%).

foaming structures are observed at 130 and 150°C, respectively. It shows that HGBs are almost broken at 130°C [Fig. 1(a)], whereas desirable embryo-foaming morphology is carried out at 150°C [Fig. 1(b)]. Based on the viscosity of LDPE with different temperature, at constant rotor speed, the viscosity of melt LDPE decreased from 130 to 150°C (in Fig. 2). Because the viscosity of ambient melt around HGB have a great effect on the tension of the HGB.

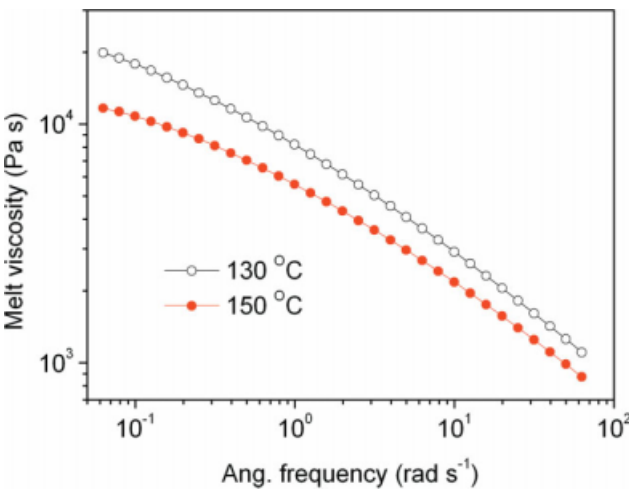

Figure 2 Angular frequency dependence of the melt viscosity for the LDPE melt with different temperature. [Color figure can be viewed in the online issue, which is available at www.interscience.wiley.com.]

Increasing melt viscosity, the LDPE melt press inner HGBs so hard that they broke. At 150°C, the HGBs in melt are intact and disperse homogeneously into the melt LDPE matrix. Such embryo-foaming morphology, i.e., intact HGB embedded homogeneously in LDPE melt, results in the formation of gas nuclei for microcellular materials, which is crucial for the following procedure of compression molding.

Forming of microcellular structure in compression molding

The effect of compression pressure on the morphology of LDPE/HGB is studied at the constant compression temperature of 160°C, as seen in Figure 3. In comparison with the premixed stage, no extra shear heat produced during the procedure of compression molding. The compression temperature is fixed at 160°C, higher than premixed temperature. The resulting morphologies of LDPE/HGB without crosslink are observed at the compression molding pressure of 6 and 8 MPa. At low processing pressure of 6 MPa, most of HGBs still keep unbroken sphere, and no N_2 releases from HGB. It shows gas nuclei cannot be formed in melt LDPE [in Fig. 3(a)]. In the other case, as shown in Figure 3(b), at 8 MPa, HGBs are almost broken, which pushed the formation of gas nuclei. However, desirable microcellular

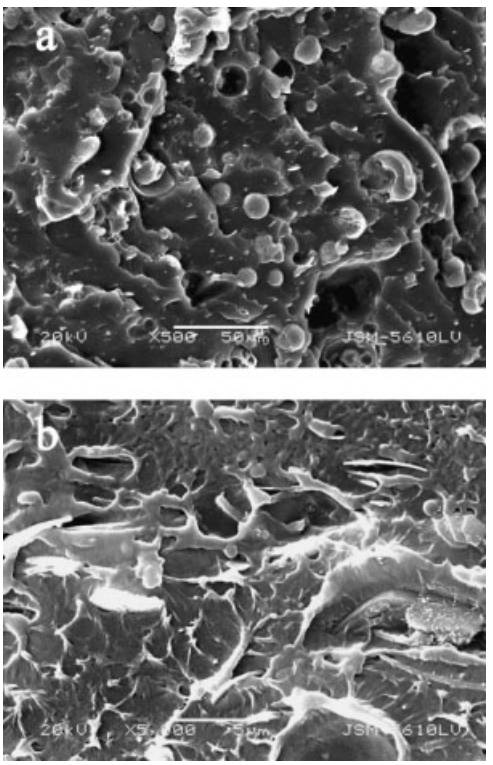

Figure 3 SEM images of HDPE/HGB in compression molding stage at pressure of (a) 6 MPa and (b) 8 MPa (f_{HGB}: 10%, 160°C, without DCP, the premixed temperature of 150 °C).

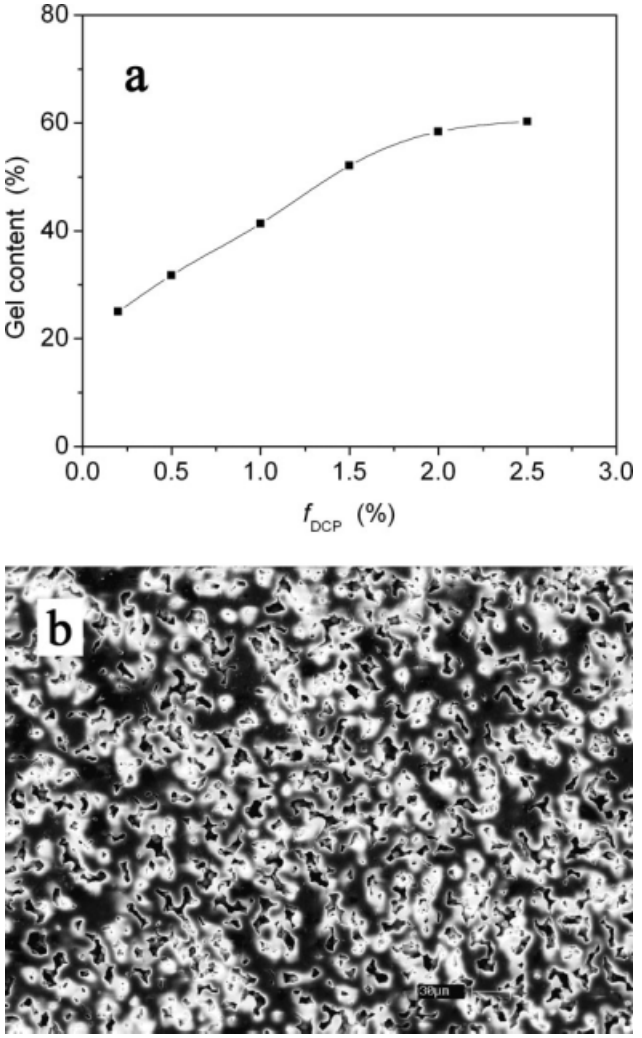

Figure 4 (a) Effect of gel content of LDPE/HGB on f_{DCP} and (b) SEM image of final HDPE/HGB microstructure (8 MPa, f_{HGB}: 10%, 160°C, f_{DCP}: 2%, the premixed temperature of 150 °C).

structure was not yet achieved. It is the reason that the melt viscosity decreases with increasing compression pressure at constant temperature, and the release of N_2 from the broken HGB induces more pronounced plastic fluxion of LDPE matrix, which results in the irrestraining growth of bubbles. Therefore, in this case, these bubbles growth have to be further immobilized for final-foaming structure.

Immobilized final cellular structure

Crosslink is an effective way to restrain plasticize distortion of polymer matrix. It can be showed the effect of gel content of crosslink LDPE/HGB on loading DCP (f_{DCP}) in Figure 4(a). At f_{DCP} is $< 2\%$, the gel content of LDPE is almost increasing linearly with f_{DCP}. When much more DCP are loaded in mixture, the content of gel does not increase distinctly. It suggests that 2% DCP adding in LDPE/HGB melt is suitable to immobilize the final microcellular structure of LDPE/HGB.

It can be observed the final microcellular structure of foaming LDPE/HGB with 2% DCP in Figure 4(b), in which most of microcellular exhibit a size of around 0.1–10 μm in diameter and the foam density is about 10^9–10^{11} cells/cm^3. In this case, the cell structure of microcellular LDPE is irregular, which is different with the traditional foam materials. N_2-filled HGBs are blowing in a several different direction depended on the structure defect of HGBs. Glass fragments from broken HGBs construct a barrier against the releasing of overfull N_2. It is the unique character of such microcellular LDPE. Because of the glass barrier and the crosslink structure induced by DCP, the bubble growth are effective restrained, accordingly, the microcellular LDPE with irregular and close cells is forming.

By controlling the embryo-foaming morphology in premixed stage and the final-foaming structure in compression molding, microcellular LDPE are obtained by using N_2-filled HGB as novel gas carriers in compression molding.

Foamed mechanism of microcellular LDPE by compression molding method

Different from traditional foaming with supercritical carbon dioxide as a blowing agent, in this case, unique foaming mechanism can be proposed, which include three steps, the formation of homogeneous gas nuclei, the growth of bubbles, and the immobilization of bubbles.

Unbroken N_2-filled HGBs are dispersed homogeneously in LDPE melt, which produce desirable embryo-foaming microstructure. Such structures incubate the formation of homogeneous gas nuclei. With the increasing compression pressure, HGBs are

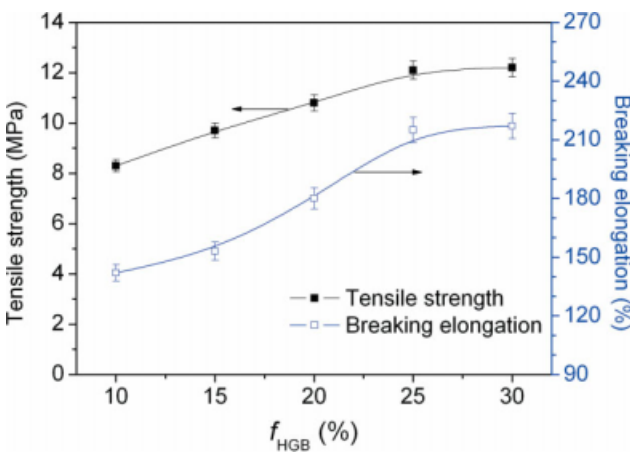

Figure 5 Tensile strength and breaking elongation of microcellular LDPE with the content of HGBs. [Color figure can be viewed in the online issue, which is available at www.interscience.wiley.com.]

TABLE I
The Charpy Nonnotch Impact Strength of Microcellular LDPE

The weight fraction of HGB (%)	10	15	20	25	30
Impact strength (MPa)	Unfractured	Unfractured	Unfractured	74.1	60.8

broken successively. N_2 released from HGB is acted as homogeneous gas nuclei. Increasing N_2 cause higher gas concentrated and LDPE melt tend to supersaturation. As the compression pressure is released and the mold are cooling down, the solubility of N_2 in melt decreased rapidly, which induce the growth of bubble nucleation center and resulted in consequently phase separation. At the same time, DCP is initiated at the processing temperature, and LDPE chains are induced to crosslink. Within the split second, the growth of bubbles retard and the immobilization of bubbles are carried out by broken HGB and crosslink polymer matrix. Therefore, it is important for the formation of microcellular structure that the homogeneous gas nuclei grow evenly up to the bubble nucleation centers and end timely in small close microcellular.

Performance of microcellular LDPE

Mechanical properties

At the constant content of 2% DCP adding in LDPE/HGB, the tensile property and impact strength of microcellular LDPE are shown in Figure 5 and Table I. With the increasing of loading HGB, the tensile strength and breaking elongation increase. The tensile strength of microcellular LDPE exceeds that of pure LDPE (9 MPa), which attribute to the rigid HGB fillers and the crosslink structure of microcellular LDPE. Because of the same reason, the breaking elongation of microcellular LDPE is lower than that of pure LDPE (600%). Therefore, the microcellular LDPE exhibits an excellent tensile property when the content of HGB ranges from 10 to 30%.

In Table I, the Charpy nonnotch impact strength can be observed. It shows that the microcellular LDPE cannot be fractured when the weight fraction of HGB are 10, 15, and 20%. Increasing the weight fraction of HGB to above 25%, the impact strength of microcellular LDPE is still beyond 60 MPa. It is demonstrate that microcellular LDPE possess excellent impact resistance.

Density, hardness, and water absorption

The density and hardness of microcellular LDPE with the content of HGB are recorded in Figure 6. Increasing the content of HGB, the density and the hardness of the microcellular LDPE are linear decreasing. As the content of HGB is 30%, the density of microcellular LDPE reaches 0.75 g/cm^3 and the hardness of microcellular LDPE keep about 93–95 as f_{HGB} ranges from 10 to 30%.

Figure 7 presents the water absorption of microcellular LDPE with the content of HGBs. As the content of HGB range from 10 to 30%, the water absorption of microcellular LDPE is as low as 0.07. As mentioned earlier, Figure 4(b) is shown, close cells existed in LDPE matrix and broken HGBs are like a hydrophobic barrier to interfere the water absorption

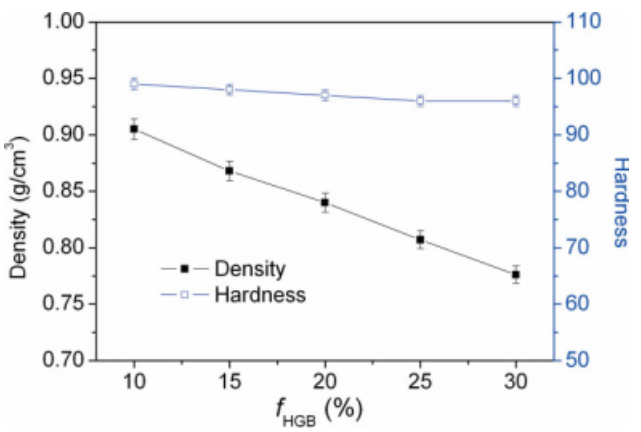

Figure 6 Density and hardness of microcellular LDPE with the content of HGBs. [Color figure can be viewed in the online issue, which is available at www.interscience.wiley.com.]

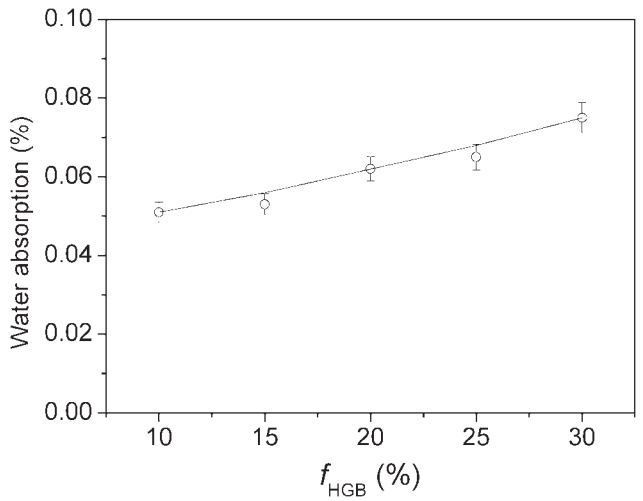

Figure 7 Water absorption of HGB of microcellular LDPE with the content of HGBs.

TABLE II
The Thermal Conductivity of LDPE/HGB Composites

Number	LDPE/HGB/DCP	Thermal conductivity (W/m K)
1	100/0/0	0.335
2	100/10/0	0.142
3	100/25/0	0.131
4	100/25/0.2	0.102
5	100/25/1.0	0.076
6	100/25/2.0	0.030

of cells. It is the reason that microcellular LDPE exhibit low water absorption.

Thermal conductivity

Microcellular structures of polymers contribute to enhancing heat distortion of polymer matrix, which is aiming at the application for heat-insulation building materials. The thermal conductivities of microcellular LDPE are shown in Table II. It shows that the thermal conductivity of LDPE/HGB composites without DCP decreased with the increasing f_{HGB}, which attribute to the own heat insulation of N_2-filled HGBs. With loading DCP, crosslink LDPE shows low thermal conductivity than that without DCP. At $f_{DCP} = 2.0\%$, the thermal conductivity of microcellular LDPE is low to 0.03 W/m K, which reaches the design standard for energy efficiency of residential buildings.

Because of the good mechanical strength, low density, weak water-absorption, and excellent heat insulate ability, microcellular LDPE will be a robust candidate as one of the best promising energy building materials.

CONCLUSION

By using N_2-filled HGB as gas carriers, microcellular LDPE is obtained by compression molding method. The average cell size ranges from 0.1 to 10 μm in diameter, and foam density is about 10^9–10^{11} cells/cm^3. The controlled micromorphologies of composites are carried out by tuning key processing parameters. Based on embryo-foaming morphology and final-foaming structure, the pertinent foaming mechanism is proposed, which include the formation of homogeneous gas nuclei, the growth and the immobile of bubble. Desirable microcellular structure of LDPE/HGB exhibit the good mechanical strength, low density and water absorption, and excellent heat insulate ability. Microcellular LDPE can be used as a robust candidate of the promising energy material in building applications.

Reference

1. Baldwin, D. F.; Park, C. B.; Suh, N. P. Polym Eng Sci 1996, 36, 1437.
2. McKeown, N. B.; Budd, P. M.; Book, D. Macromol Rapid Commun 2007, 28, 995.
3. Siripurapu, S.; Desimone, J. M.; Khan, S. A.; Spontak, R. J. Adv Mater 2004, 16, 989.
4. Youn, J. R.; Suh, N. P. Polym Compos 1985, 6, 175.
5. Kim, K. Y.; Kang, S. L.; Kwak, H. Polym Eng Sci 2004, 44, 1980.
6. Kwak, H.; Lee, S. J Heat Transfer 1991, 113, 714.
7. Octoby, D. W. J Phys: Condens Matter 1992, 4, 7627.
8. Han, J. H.; Han, C. D. J Polym Sci Part B: Polym Phys 1990, 28, 743.
9. Lee, J. G.; Flumerfelt, R. W. J Colloid Interface Sci 1996, 184, 335.
10. Kwak, H.; Panton, R. L. J Chem Phys 1983, 78, 5795.
11. Kwak, H.; Panton, R. L. J Phys D: Appl Phys 1985, 18, 647.
12. Epstein, P. S; Plesset, M. S. J Chem Phys 1950, 18, 1505.
13. Scriven, L. E. Chem Eng Sci 1959, 10, 1.
14. Han, C. D.; Yoo, H. J. Polym Eng Sci 1981, 21, 518.
15. Shafi, M. A.; Joshi, K. R.; Flumerfelt, W. Chem Eng Sci 1997, 52, 635.
16. Joshi, K.; Lee, J. G.; Shafi, M. A.; Flumerfelt, R. W. J Appl Polym Sci 1998, 67, 1353.
17. Bledzki, A. K.; Faruk O. J Appl Polym Sci 2005, 97, 1090.
18. Tsivintzelis I.; Angelopoulou, A. G.; Panayiotou, C. Polymer 2007, 48, 5928.
19. Kaewmesri, W.; Rachtanapun, P.; Pumchusak, J. J Appl Polym Sci 2008, 107, 63.
20. Yakisir, D.; Mighri, F.; Bousmina, M. Macromol Rapid Commun 2006, 27, 1596.
21. Huang, H.; Wang, J. J Appl Polym Sci 2007, 106, 505.
22. Liu, Y.; Wu, D. M.; Long, W. B.; Xu, S. H.; Wu, G. F.; Wu, M. Plastics 1996, 25, 45.